

Exponential B-spline Collocation Solutions to the Gardner Equation

Ozlem Ersoy Hepson^{a,*}, Alper Korkmaz^b, Idiris Dag^c

^a *Eskisehir Osmangazi University, Mathematics & Computer Department, Eskisehir, Turkey,*

^b *Çankırı Karatekin University, Department of Mathematics, Çankırı, Turkey,*

^c *Eskisehir Osmangazi University, Computer Engineering Department, Eskisehir, Turkey.*

Abstract

The exponential B-spline basis function set is used to develop a collocation method for some initial boundary value problems (IBVPs) to the Gardner equation. The Gardner equation has two nonlinear terms, namely quadratic and cubic ones. The order reduction of the equation is resulted in a coupled system of PDEs that enables the exponential B-splines to be implemented. The system is integrated in time by Crank-Nicolson implicit method. The validity of the method is investigated by calculating the discrete maximum error norm and observing the absolute relative changes of the conservation laws at the end of the simulations.

Keywords: Gardner equation, soliton, interaction, wave generation, exponential B-spline.

1. Introduction

The Gardner equation

$$u_t + \mu_1 u u_x + \mu_2 u^2 u_x + \mu_3 u_{xxx} = 0 \quad (1)$$

where $\mu_i, i = 1, 2, 3$ are constant parameters has two nonlinear terms besides the third order dissipative term. When these two nonlinear terms are considered, the equation is a combined form of the Korteweg-de Vries and the modified Korteweg-de Vries equations. The Gardner equation is a significant model for the motion of negative ion-acoustic plasma waves [1]. The equation can also describe internal waves with large amplitudes and weakly nonlinear dispersive waves [2]. Moreover, undular bore type solutions for the Gardner equation and the relation of

Email address: ozersoy@ogu.edu.tr (Ozlem Ersoy Hepson^{a,*}, Alper Korkmaz^b, Idiris Dag^c)

these solutions with the sign of the cubic nonlinear term are studied in details by Kamchatnov et al. in the same paper. Various patterns covering undular bores in the bright and dark cnoidals, trigonometric bores, kinks and some other types constructed from them are developed in [2]. Occurrence of large ocean waves in unexpected meaning can be modeled by in the Gardner equation and in some cases the modulational instability can be observed [3]. An analytical study deals with transcritical flow of a fluid passing a local topographical obstacle [4].

Interaction of various types of solitons and other wave profiles are examined in details in different studies. Collision of a large amplitude soliton with a limiting soliton is derived by the aid of the Darboux transformation [5]. A large class of interaction solutions of solitons with cnoidal and periodic waves is constructed by the consistent tanh-expansion method [6]. Some collusion models of cnoidal wave to soliton are derived by the consistent Riccati expansion approach [7]. Some exact traveling wave type solutions constructed in terms of tanh and coth are constructed by implementing the extended form of the tanh method [8]. Projective Riccati equations also enable to generate some hyperbolic type solitary wave and periodic solutions expressed in the finite series form [9]. These type solutions can also be constructed by generalized form of the (G'/G) -expansion [10, 11, 12], exp – function [13] methods. A bunch of traveling wave type exact solutions to the Gardner equation are determined by using various hyperbolic ansatzes[14]. Zayed and Abdelaziz [15] focus on new exact traveling wave solutions constructed by $(G'/G, 1/G)$ approach. Mapping method can also be used to integrate the Gardner equation [16]. Lie group and tan-cot methods are also effective methods to construct some exact solutions to the Gardner equation [17, 18].

The three conservation laws representing various physical quantities such as momentum, energy and etc. are given for the generalized Gardner equation power law nonlinearities by using some algebraic and derivative manipulations [19]. Some finite difference and restrictive Taylor's approximation are used to determine the numerical solutions to the Gardner equation [20, 21]. In the present study, we construct exponential B-spline collocation algorithms for the numerical solutions to some IBVPs for the Gardner equation. Even though the cubic degree of the basis does not allow to approach the third order derivative, the reduction of the derivative order permits to implement of the method to the resultant nonlinear PDE system.

Let $v = u_x$. Then, the Gardner equation (1) is reduced to a coupled system nonlinear PDEs

$$\begin{aligned} u_t + (\mu_1 u + \mu_2 u^2) u_x + \mu_3 v_{xx} &= 0 \\ v - u_x &= 0 \end{aligned} \tag{2}$$

The initial data

$$\begin{aligned} u(x, 0) &= \omega(x) \\ v(x, 0) &= \omega_x(x) \end{aligned} \quad (3)$$

and the zero Neumann conditions at both end of the artificial finite problem interval $[a, b]$ are combined with the system (2) for the mathematical representation of the IBVPs.

2. Exponential B-spline Approach

Let π be a uniformly distributed grids of the finite interval $[a, b]$, such as,

$$\pi : x_m = a + mh, m = 0, 1, \dots, N$$

where $h = \frac{b-a}{N}$. Then, the exponential cubic B-splines set

$$B_m(x) = \begin{cases} b_2 \left((x_{m-2} - x) - \frac{1}{\zeta} \sinh(\zeta(x_{m-2} - x)) \right) & , \quad [x_{m-2}, x_{m-1}] \\ a_1 + b_1(x_m - x) + c_1 \exp(\zeta(x_m - x)) + d_1 \exp(-\zeta(x_m - x)) & , \quad [x_{m-1}, x_m] \\ a_1 + b_1(x - x_m) + c_1 \exp(\zeta(x - x_m)) + d_1 \exp(-\zeta(x - x_m)) & , \quad [x_m, x_{m+1}] \\ b_2 \left((x - x_{m+2}) - \frac{1}{\zeta} \sinh(\zeta(x - x_{m+2})) \right) & , \quad [x_{m+1}, x_{m+2}] \\ 0 & , \quad \textit{otherwise} \end{cases} \quad (4)$$

where $m = -1, 0, \dots, N + 1$,

$$\begin{aligned} a_1 &= \frac{\zeta h \cosh(\zeta h)}{\zeta h \cosh(\zeta h) - \sinh(\zeta h)}, \\ b_1 &= \frac{\zeta \cosh(\zeta h)(\cosh(\zeta h) - 1) + \sinh^2(\zeta h)}{2(\zeta h \cosh(\zeta h) - \sinh(\zeta h))(1 - \cosh(\zeta h))}, \\ b_2 &= \frac{\zeta}{2(\zeta h \cosh(\zeta h) - \sinh(\zeta h))}, \\ c_1 &= \frac{1 \exp(-\zeta h)(1 - \cosh(\zeta h)) + \sinh(\zeta h)(\exp(-\zeta h) - 1)}{4(\zeta h \cosh(\zeta h) - \sinh(\zeta h))(1 - \cosh(\zeta h))}, \\ d_1 &= \frac{1 \exp(\zeta h)(\cosh(\zeta h) - 1) + \sinh(\zeta h)(\exp(\zeta h) - 1)}{4(\zeta h \cosh(\zeta h) - \sinh(\zeta h))(1 - \cosh(\zeta h))}, \end{aligned}$$

with real parameter ζ constitutes a basis functions set for the functions defined over the problem interval $[a, b]$ [22]. Each exponential cubic B-spline $B_m(x)$ has two continuous first and second order derivatives defined in the interval $[x_{m-2}, x_{m+2}]$. Exponential B-splines are used as basis functions in some methods to solve problems appearing in various fields [23, 24, 25, 26, 27, 28]. The functional and derivative values of the exponential B-splines are summarized in Table 1 .

Table 1: $B_m(x)$ and its first and second derivatives

x	x_{m-2}	x_{m-1}	x_m	x_{m+1}	x_{m+2}
B_m	0	$\frac{\sinh(\zeta h) - \zeta h}{2(\zeta h \cosh(\zeta h) - \sinh(\zeta h))}$	1	$\frac{\sinh(\zeta h) - \zeta h}{2(\zeta h \cosh(\zeta h) - \sinh(\zeta h))}$	0
B'_m	0	$\frac{\zeta(1 - \cosh(\zeta h))}{2(\zeta h \cosh(\zeta h) - \sinh(\zeta h))}$	0	$\frac{\zeta(\cosh(\zeta h) - 1)}{2(\zeta h \cosh(\zeta h) - \sinh(\zeta h))}$	0
B''_m	0	$\frac{\zeta^2 \sinh(\zeta h)}{2(\zeta h \cosh(\zeta h) - \sinh(\zeta h))}$	$-\frac{\zeta^2 \sinh(\zeta h)}{\zeta h \cosh(\zeta h) - \sinh(\zeta h)}$	$\frac{\zeta^2 \sinh(\zeta h)}{2(\zeta h \cosh(\zeta h) - \sinh(\zeta h))}$	0

Let U and V be approximate solutions to u and v respectively. Then,

$$U(x, t) = \sum_{m=-1}^{N+1} \delta_m B_m(x), \quad V(x, t) = \sum_{m=-1}^{N+1} \phi_m B_m(x). \quad (5)$$

where δ_m and ϕ_m are time dependent parameters to be determined from the collocation points $x_m, m = 0, \dots, N$ and the complementary data. The nodal values U and its first and second derivatives at the knots can be found from the (5) as

$$\begin{aligned} U_m = U(x_m, t) &= \frac{s - \zeta h}{2(\zeta h c - s)} \delta_{m-1} + \delta_m + \frac{s - \zeta h}{2(\zeta h c - s)} \delta_{m+1}, \\ U'_m = U'(x_m, t) &= \frac{\zeta(1 - c)}{2(\zeta h c - s)} \delta_{m-1} + \frac{\zeta(c - 1)}{2(\zeta h c - s)} \delta_{m+1} \end{aligned} \quad (6)$$

$$\begin{aligned} U''_m = U''(x_m, t) &= \frac{\zeta^2 s}{2(\zeta h c - s)} \delta_{m-1} - \frac{\zeta^2 s}{\zeta h c - s} \delta_m + \frac{\zeta^2 s}{2(\zeta h c - s)} \delta_{m+1} \\ V_m = V(x_m, t) &= \frac{s - \zeta h}{2(\zeta h c - s)} \phi_{m-1} + \phi_m + \frac{s - \zeta h}{2(\zeta h c - s)} \phi_{m+1}, \\ V'_m = V'(x_m, t) &= \frac{\zeta(1 - c)}{2(\zeta h c - s)} \phi_{m-1} + \frac{\zeta(c - 1)}{2(\zeta h c - s)} \phi_{m+1} \end{aligned} \quad (7)$$

$$V''_m = V''(x_m, t) = \frac{\zeta^2 s}{2(\zeta h c - s)} \phi_{m-1} - \frac{\zeta^2 s}{\zeta h c - s} \phi_m + \frac{\zeta^2 s}{2(\zeta h c - s)} \phi_{m+1}.$$

When Gardner equation is space-splitted as (2), the resultant system has maximum second order derivatives that enables to construct a smooth cubic B-spline approximation with the exponential B-splines. Implementation of the Crank-Nicolson method to the space-splitted system (2) yields

$$\begin{aligned} \frac{U^{n+1} - U^n}{\Delta t} + \mu_1 \frac{(UU_x)^{n+1} + (UU_x)^n}{2} + \mu_2 \frac{(U^2 U_x)^{n+1} + (U^2 U_x)^n}{2} + \mu_3 \frac{V_{xx}^{n+1} + V_{xx}^n}{2} &= 0 \\ \frac{V^{n+1} + V^n}{2} - \frac{U_x^{n+1} + U_x^n}{2} &= 0 \end{aligned} \quad (8)$$

where $t^{n+1} = t^n + \Delta t$, and the superscripts n and $n+1$ denote (n) th and $(n+1)$ th time levels, respectively.

The nonlinear terms $(UU_x)^{n+1}$ and $(U^2U_x)^{n+1}$ in Eq. (8) are converted to linear forms by using

$$(UU_x)^{n+1} = U^{n+1}U_x^n + U^nU_x^{n+1} - U^nU_x^n$$

and

$$(U^2U_x)^{n+1} = 2U^{n+1}U^nU_x^n + (U^n)^2U_x^{n+1} - 2(U^n)^2U_x^n$$

defined in [29]. The resultant linear system is discretized in time by using Crank-Nicolson method as

$$\begin{aligned} & \left[\left(\frac{2}{\Delta t} + \mu_1 L + 2\mu_2 KL \right) \alpha_1 + (\mu_1 K + \mu_2 K^2) \beta_1 \right] \delta_{j-1}^{n+1} + [\mu_3 \gamma_1] \phi_{j-1}^{n+1} + \left[\left(\frac{2}{\Delta t} + \mu_1 L + 2\mu_2 KL \right) \alpha_2 \right] \delta_j^{n+1} \\ & + [\mu_3 \gamma_2] \phi_j^{n+1} + \left[\left(\frac{2}{\Delta t} + \mu_1 L + 2\mu_2 KL \right) \alpha_1 - (\mu_1 K + \mu_2 K^2) \beta_1 \right] \delta_{j+1}^{n+1} + [\mu_3 \gamma_1] \phi_{j+1}^{n+1} \\ & = \left[\left(\frac{2}{\Delta t} + \mu_2 KL \right) \alpha_1 \right] \delta_{j-1}^n - \mu_3 \gamma_1 \phi_{j-1}^n + \left[\left(\frac{2}{\Delta t} + \mu_2 KL \right) \alpha_2 \right] \delta_j^n - \mu_3 \gamma_2 \phi_j^n + \left[\left(\frac{2}{\Delta t} + \mu_2 KL \right) \alpha_1 \right] \delta_{j+1}^n - \mu_3 \gamma_1 \phi_{j+1}^n \\ & - \beta_1 \delta_{j-1}^{n+1} + \alpha_1 \phi_{j-1}^{n+1} + \alpha_2 \phi_j^{n+1} + \beta_1 \delta_{j+1}^{n+1} + \alpha_1 \phi_{j+1}^{n+1} = \beta_1 \delta_{j-1}^n - \alpha_1 \phi_{j-1}^n - \alpha_2 \phi_j^n - \beta_1 \delta_{j+1}^n - \alpha_1 \phi_{j+1}^n \\ & m = 0, \dots, N, \quad n = 0, 1, \dots, \end{aligned} \tag{9}$$

where

$$\begin{aligned} K &= \alpha_1 \delta_{m-1}^n + \delta_m^n + \alpha_1 \delta_{m+1}^n \\ L &= \alpha_1 \phi_{m-1}^n + \phi_m^n + \alpha_1 \phi_{m+1}^n \end{aligned}$$

$$\begin{aligned} \alpha_1 &= \frac{s - \zeta h}{2(\zeta hc - s)}, \\ \gamma_1 &= \frac{\zeta^2 s}{2(\zeta hc - s)}, \quad \gamma_2 = -\frac{\zeta^2 s}{\zeta hc - s} \\ \beta_1 &= \frac{\zeta(1-c)}{2(\zeta hc - s)}, \quad \beta_2 = \frac{\zeta(c-1)}{2(\zeta hc - s)} \end{aligned}$$

The system (9) can be rewritten in the matrix form as

$$\mathbf{Ax}^{n+1} = \mathbf{Bx}^n \tag{10}$$

where

$$\mathbf{A} = \begin{bmatrix} \nu_{m1} & \nu_{m2} & \nu_{m3} & \nu_{m4} & \nu_{m5} & \nu_{m2} & & & & \\ -\beta_1 & \alpha_1 & 0 & \alpha_2 & \beta_1 & \alpha_1 & & & & \\ & & \nu_{m1} & \nu_{m2} & \nu_{m3} & \nu_{m4} & \nu_{m5} & \nu_{m2} & & \\ & & -\beta_1 & \alpha_1 & 0 & \alpha_2 & \beta_1 & \alpha_1 & & \\ & & & \ddots & \ddots & \ddots & \ddots & \ddots & \ddots & \\ & & & & \nu_{m1} & \nu_{m2} & \nu_{m3} & \nu_{m4} & \nu_{m5} & \nu_{m2} \\ & & & & -\beta_1 & \alpha_1 & 0 & \alpha_2 & \beta_1 & \alpha_1 \end{bmatrix}$$

3. Stability Analysis

The stability of the method is investigated by performing the Von-Neumann analysis where

$$\begin{aligned}\delta_j^n &= A_1 \xi^n \exp(ij\varphi) \\ \phi_j^n &= A_2 \xi^n \exp(ij\varphi)\end{aligned}\quad (12)$$

$$\rho = \frac{\xi^{n+1}}{\xi^n}$$

Here, A_1 and A_2 represent the harmonics amplitude. k is the mode number, ρ is the amplification factor and $\varphi = kh$. The term $U + U^2$ is assumed as locally constant and replaced ε . Substituting 12 into the system

$$\begin{aligned}& a_1 \delta_{j-1}^{n+1} + a_2 \delta_j^{n+1} + a_1 \delta_{j+1}^{n+1} + \frac{\lambda k \varepsilon}{2} (a_3 \delta_{j-1}^{n+1} - a_3 \delta_{j+1}^{n+1}) + \frac{k \mu_3}{2} (a_4 \phi_{j-1}^{n+1} + a_5 \phi_j^{n+1} + a_4 \phi_{j+1}^{n+1}) \\ &= a_1 \delta_{j-1}^n + a_2 \delta_j^n + a_1 \delta_{j+1}^n - \frac{\lambda k \varepsilon}{2} (a_3 \delta_{j-1}^n - a_3 \delta_{j+1}^n) - \frac{k \mu_3}{2} (a_4 \phi_{j-1}^n + a_5 \phi_j^n + a_4 \phi_{j+1}^n) \\ & \quad a_3 \delta_{j-1}^{n+1} - a_3 \delta_{j+1}^{n+1} - a_1 \phi_{j-1}^{n+1} - a_2 \phi_j^{n+1} - a_1 \phi_{j+1}^{n+1} \\ &= -a_3 \delta_{j-1}^n + a_3 \delta_{j+1}^n + a_1 \phi_{j-1}^n + a_2 \phi_j^n + a_1 \phi_{j+1}^n\end{aligned}\quad (14)$$

gives

$$\begin{aligned}& \xi^{n+1} \left[A_1 (2a_1 \cos \varphi + a_2) + \frac{A_2 k \mu_3}{2} (2a_4 \cos \varphi + a_5) - i \lambda k \varepsilon A_1 a_3 \sin \varphi \right] \\ &= \xi^n \left[A_1 (2a_1 \cos \varphi + a_2) - \frac{A_2 k \mu_3}{2} (2a_4 \cos \varphi + a_5) - i \lambda k \varepsilon A_1 a_3 \sin \varphi \right] \\ & \frac{\xi^{n+1}}{\xi^n} = \frac{[A_1 (2a_1 \cos \varphi + a_2) - \frac{A_2 k \mu_3}{2} (2a_4 \cos \varphi + a_5) - i \lambda k \varepsilon A_1 a_3 \sin \varphi]}{[A_1 (2a_1 \cos \varphi + a_2) + \frac{A_2 k \mu_3}{2} (2a_4 \cos \varphi + a_5) - i \lambda k \varepsilon A_1 a_3 \sin \varphi]} \\ & \rho = \frac{\xi^{n+1}}{\xi^n} = \frac{X_1 + iY}{X_2 - iY}\end{aligned}\quad (15)$$

where

$$\begin{aligned}X_1 &= A_1 (2a_1 \cos \varphi + a_2) - \frac{A_2 k \mu_3}{2} (2a_4 \cos \varphi + a_5) \\ X_2 &= A_1 (2a_1 \cos \varphi + a_2) + \frac{A_2 k \mu_3}{2} (2a_4 \cos \varphi + a_5) \\ Y &= i \lambda k \varepsilon A_1 a_3 \sin \varphi\end{aligned}$$

and

$$\begin{aligned}
& \xi^{n+1} [-A_2 (2a_1 \cos \varphi + a_2) - 2iA_1 a_3 \sin \varphi] \\
&= \xi^n [A_2 (2a_1 \cos \varphi + a_2) + 2iA_1 a_3 \sin \varphi] \\
\frac{\xi^{n+1}}{\xi^n} &= \frac{A_2 (2a_1 \cos \varphi + a_2) + 2iA_1 a_3 \sin \varphi}{-A_2 (2a_1 \cos \varphi + a_2) - 2iA_1 a_3 \sin \varphi} \\
\rho &= \frac{\xi^{n+1}}{\xi^n} = \frac{X_3 + iZ}{X_4 - iZ} \tag{16}
\end{aligned}$$

$$\begin{aligned}
X_3 &= A_2 (2a_1 \cos \varphi + a_2) \\
X_4 &= -A_2 (2a_1 \cos \varphi + a_2) \\
Z &= 2iA_1 a_3 \sin \varphi
\end{aligned}$$

It can be concluded from both (15) and (16) that $|\rho|$ is less than or equal to 1. Thus, the proposed method method is unconditionally stable.

4. Illustrations

This section contains implementation of the proposed algorithm to some IVPs to validate its accuracy and efficiency. The accuracy of the numerical results is measured by using the discrete maximum norm defined as

$$L_\infty(t) = |u(x, t) - U(x, t)|_\infty = \max_m |u(x_m, t) - U(x_m, t)|$$

at the time t when the analytical solution exists.

The conservation laws also validates the accuracy of the proposed algorithms if they keep their initial values even in the nonexistence of the analytical solutions case. The lowest three conservation laws

$$\begin{aligned}
M &= \int_{-\infty}^{\infty} u dx \\
E &= \int_{-\infty}^{\infty} u^2 dx \\
H &= \int_{-\infty}^{\infty} \frac{\mu_1 u^3}{3} + \frac{\mu_2 u^4}{6} - \mu_3 (u_x)^2 dx
\end{aligned} \tag{17}$$

are expected to keep their initial values as time proceeds[19]. In order to measure the absolute relative changes of these quantities at any time $t > 0$, $C(M_t)$, $C(E_t)$ and $C(H_t)$ are defined as

$$\begin{aligned} C(M_t) &= \left| \frac{M_t - M_0}{M_0} \right| \\ C(E_t) &= \left| \frac{E_t - E_0}{E_0} \right| \\ C(H_t) &= \left| \frac{H_t - H_0}{H_0} \right| \end{aligned} \tag{18}$$

where M_0 , E_0 and H_0 are initial, M_t , E_t and H_t are the quantities at the time $t > 0$.

4.1. Example 1

The solution representing the propagation of an initial positive pulse is demonstrated by using the initial condition

$$u(x, 0) = \frac{2}{12 + 3\sqrt{14} \cosh(-\frac{x}{3} + \frac{5}{3})}$$

and the homogeneous Neumann conditions at both ends of the problem interval $[-20, 30]$. The analytical solution can be written as

$$u(x, t) = \frac{2}{12 + 3\sqrt{14} \cosh(-\frac{x}{3} + \frac{5}{3} + \frac{t}{27})}$$

when the compatible parameters are chosen $\mu_1 = 4$, $\mu_2 = -3$ and $\mu_3 = 1$ in the Gardner equation (1). This solution represents propagation of a positive initial pulse along the x -axis as time proceeds. The simulation of the solution is depicted in Fig 1 in the time domain $[0, 5]$

Various discretization parameters h and Δt are used to illustrate the numerical solutions. The optimum value of exponential spline parameter ζ is scanned by comparing the discrete maximum error norms at the simulation terminating time. The maximum values of the errors are measured near the peak points as expected for both $\zeta = 1$ and $\zeta = 0.000003$. The maximum error distribution for $\zeta = 1$ and $\zeta = 0.000003$ are depicted in Fig 2(a) and Fig 2(b), respectively, for $h = 0.5$ and $\Delta t = 0.1$.

The discrete maximum error norms at some distinct times are reported in Table 2 for various values of the discretization parameter h and fixed Δt . Even though the solutions are improved when the spatial discretization parameter size is reduced when $\zeta = 1$ at both $t = 2.5$ and $t = 5$. For various values of the

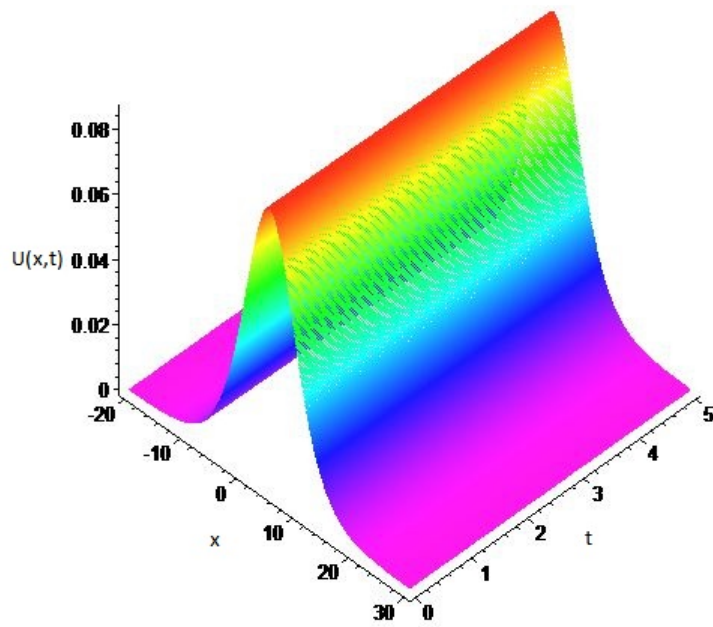
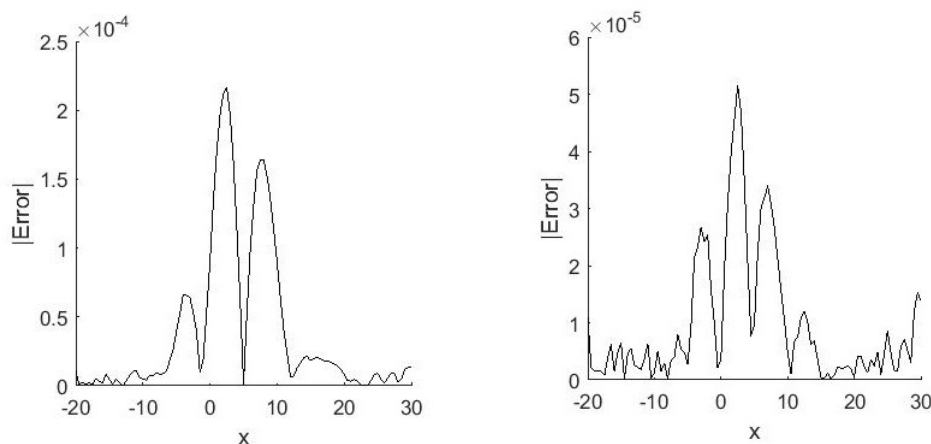


Figure 1: Propagation of initial positive pulse

spatial discretization parameter, the optimum exponential B-spline parameter is scanned to reduce the maximum error. When h is larger, the optimum ζ improves the results by decreasing the error approximately one third or one fourth. Even though the better results are obtained for smaller h values, the optimum choice of ζ increases the accuracy two times.



(a) Error distribution for $\zeta = 1$ at the simulation terminating time (b) Error distribution for $\zeta = 0.000003$ at the simulation terminating time

Figure 2: Error of the numerical error at the time $t = 5$

Table 2: L_∞ Error norms for $\mu_1 = 4$, $\mu_2 = -3$, $\mu_3 = 1$, $\Delta t = 0.1$, $t = 2.5$ and 5 , $-20 \leq x \leq 30$

N	$L_\infty(2.5)(\zeta = 1)$	$L_\infty(2.5)(\text{various } \zeta)$	$L_\infty(5)(\zeta = 1)$	$L_\infty(5)(\text{various } \zeta)$
100	1.1502×10^{-4}	($\zeta = 0.000003$) 3.2331×10^{-5}	2.1665×10^{-4}	($\zeta = 0.000003$) 5.1481×10^{-5}
200	4.1696×10^{-5}	($\zeta = 0.000001$) 1.6622×10^{-5}	5.7428×10^{-5}	($\zeta = 0.000001$) 1.8886×10^{-5}
300	2.3860×10^{-5}	($\zeta = 0.000005$) 1.3923×10^{-5}	2.9888×10^{-5}	($\zeta = 0.000004$) 1.7006×10^{-5}
400	1.6985×10^{-5}	($\zeta = 0.000004$) 1.4470×10^{-5}	1.8721×10^{-5}	($\zeta = 0.000003$) 1.5404×10^{-5}

The initial values of the conservation laws are computed with computer algebra tools and reported in Table 3. A stable numerical method is expected to preserve these values as time goes. The absolute relative changes of all related conservation laws reported in Table 3. They all are preserved at least six decimal digits for various values of h and $\zeta = 1$. The preservation of conservation laws is an indicator of a reliable numerical approach.

Table 3: Absolute relative changes of conservation laws for for $\zeta = 1$

N	M_0	E_0	H_0	$C(M_5)$	$C(E_5)$	$C(H_5)$
100	1.04458	0.06013453	0.00407022	5.5668×10^{-6}	2.6168×10^{-8}	1.2174×10^{-5}
200	1.04458	0.06013453	0.00407022	2.9640×10^{-6}	5.0740×10^{-8}	1.0597×10^{-6}
300	1.04458	0.06013453	0.00407022	2.3326×10^{-7}	2.2152×10^{-8}	2.7126×10^{-6}
400	1.04458	0.06013453	0.00407022	1.1862×10^{-6}	8.8551×10^{-10}	3.3555×10^{-6}

4.2. Example 2

The solution of the Gardner equation (1) representing the motion of kink like wave is of the form

$$u(x, t) = \frac{1}{10} - \frac{1}{10} \tanh\left(\frac{(x - \frac{t}{30})\sqrt{30}}{60}\right)$$

when the equation parameters are chosen as $\mu_1 = 1$, $\mu_2 = -5$ and $\mu_3 = 1$. The initial condition required for the numerical simulation is derived from the analytical solution by substituting $t = 0$ in the analytical solution. The homogeneous Neumann boundary conditions are used to complement the problem statement. The designed algorithm is run up to the terminating time $t = 12$ in the finite interval $[-80, 80]$. The results are graphed in Fig 3.

The maximum error distributions for $\zeta = 1$ and $\zeta = 0.000001$ are depicted in Fig 4(a) and Fig 4(b), respectively, for $N = 100$. The errors are larger around $x = 0$ as expected due to the shape of the kink like wave.

The maximum error norms are calculated for various values of N for $\zeta = 1$. In order to improve the results, the optimum value of the exponential B-spline parameter are investigated by scanning. Determination of optimum values of rho different from 1 gives at least one decimal digit better results, Table 4. Even though the results improve when N increases, optimum values of ζ improves results independent on the discretization parameters.

Table 4: L_∞ Error norms for $\mu_1 = 1$, $\mu_2 = -5$, $\mu_3 = 1$, $\Delta t = 0.1$, $t = 12$, $-80 \leq x \leq 80$

N	$L_\infty(12)(\zeta = 1)$	$L_\infty(12)(\text{various } \zeta)$
100	3.8436×10^{-4}	($\zeta = 0.000001$) 2.3022×10^{-5}
200	1.0016×10^{-4}	($\zeta = 0.000002$) 5.8623×10^{-6}
400	2.5327×10^{-5}	($\zeta = 0.000004$) 1.3684×10^{-6}
600	1.1280×10^{-5}	($\zeta = 0.000006$) 5.3420×10^{-7}
800	6.3476×10^{-6}	($\zeta = 0.000008$) 2.3800×10^{-7}

The initial values and absolute relative changes of the conservation laws are tabulated in Table 5. Absolute relative changes of all the conservation laws are calculated in four decimal digits independently on number of spatial discretization point number, Table 5.

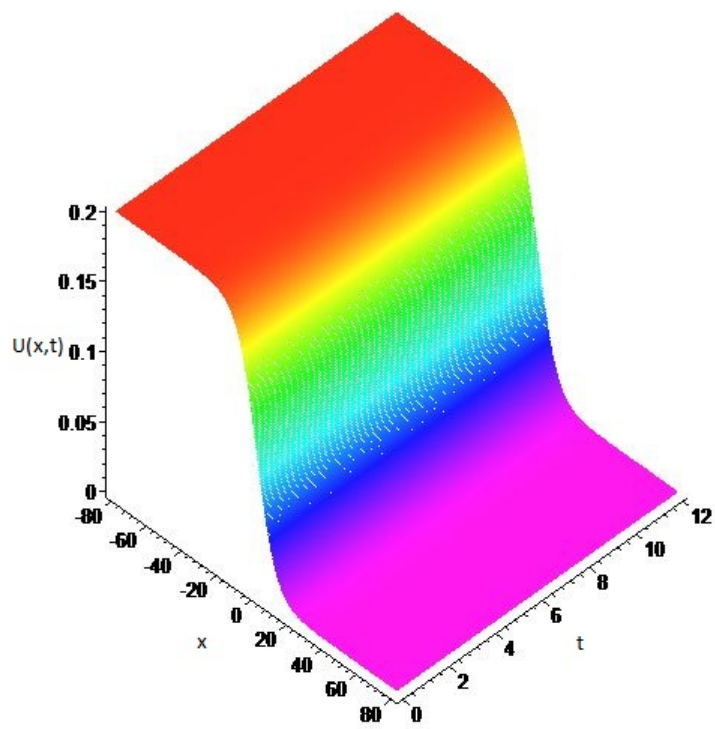
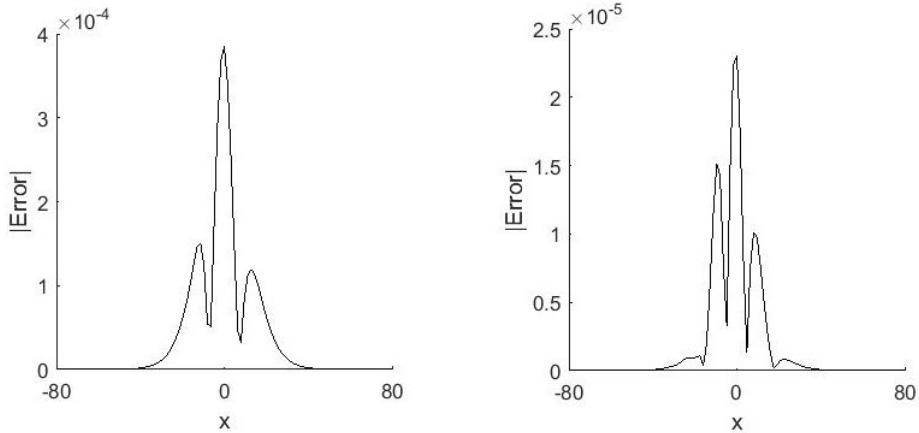


Figure 3: Motion of kink like wave



(a) Error distribution for $\zeta = 1$ at the simulation terminating time (b) Error distribution for $\zeta = 0.000001$ at the simulation terminating time

Figure 4: Error of the numerical error at the time $t = 12$

Table 5: Absolute relative changes of lowest three conservation laws for $\zeta = 1$

N	M_0	E_0	H_0	$C(M_{12})$	$C(E_{12})$	$C(H_{12})$
100	16.1599	3.0129	0.0979	4.9493×10^{-4}	5.3092×10^{-4}	5.4405×10^{-4}
200	16.0799	2.9969	0.0974	4.9750×10^{-4}	5.3387×10^{-4}	5.4720×10^{-4}
400	16.0399	2.9889	0.0971	4.9875×10^{-4}	5.3531×10^{-4}	5.4871×10^{-4}
600	16.0266	2.9862	0.0971	4.9917×10^{-4}	5.3578×10^{-4}	5.4922×10^{-4}
800	16.0199	2.9849	0.0970	4.9937×10^{-4}	5.3602×10^{-4}	5.4947×10^{-4}

4.3. Example 3

The wave generation from an initial positive pulse is studied as the last example. The initial condition used in the first example is perturbed carefully to generate new waves. Thus, an initial condition is produced for $\mu_1 = 10$, $\mu_2 = -3$ and $\mu_3 = 1$ as

$$u(x, 0) = \frac{2}{3} \frac{5}{4 + \sqrt{14} \cosh\left(\frac{x}{3} - \frac{5}{3}\right)}$$

This initial pulse is expected to generate new pulses behind as propagating towards to the right along the horizontal axis. The numerical simulation is accomplished with the discretization parameters $h = 0.5$ and $\Delta t = 0.1$ in the interval $[-40, 60]$. The simulation is depicted in Fig 5(a) - 5(d).

The initial values and the absolute relative changes of the conservation laws are recorded during the simulation process duration in Table 6. It is clearly observable that all the conservation laws are preserved successfully at least three decimal digits in the simulation period.

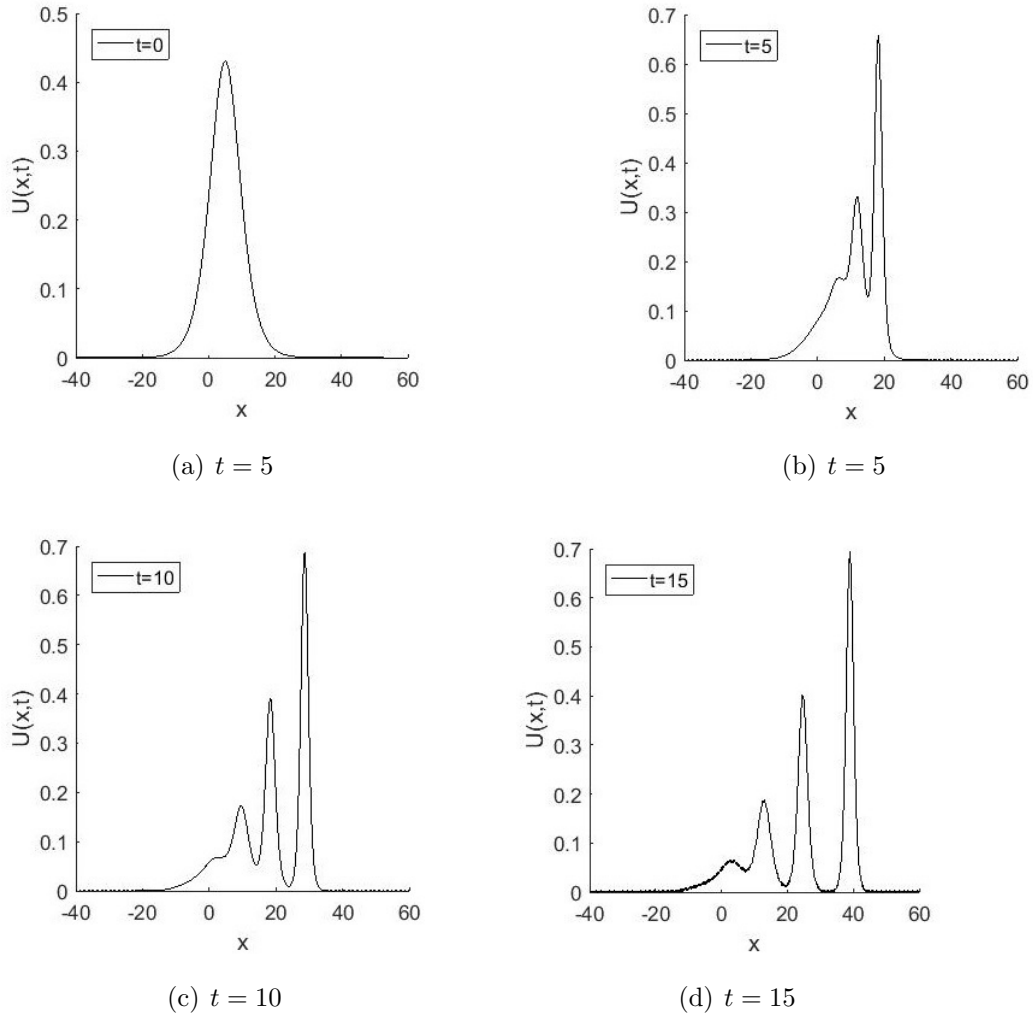


Figure 5: Wave generation simulation

Table 6: Absolute relative changes of lowest three conservation laws for for $\zeta = 1$

t	M_0	E_0	H_0	$C(M_t)(p=1)$	$C(E_t)(p=1)$	$C(H_t)(p=1)$
5	5.2255	1.5033	1.5994	1.2040×10^{-6}	3.7180×10^{-5}	21608×10^{-3}
10	5.2255	1.5033	1.5994	3.6819×10^{-6}	5.2527×10^{-5}	3.1907×10^{-3}
15	5.2255	1.5033	1.5994	8.9144×10^{-6}	5.8526×10^{-4}	3.5478×10^{-3}

5. Conclusion

The exponential B-spline collocation method is implemented for IBVPs with analytical and non analytical solutions. Having no continuous third order derivative of exponential B-splines forces us to reduce the order of third order derivative term. Thus, the Gardner equation reduces to a coupled nonlinear PDE system with maximum second order derivative term. The exponential B-spline approach to the solution of this system is substituted into the system following the Crank-Nicolson implicit time integration method. Linearization of both non linear terms with quadratic and cubic nonlinearities is followed by implementation of boundary data to obtain a solvable system of equation having equal numbers of equations and unknowns. The algorithm gets ready to run after arranging the initial state by the aid of initial and boundary data.

The validity of the method is checked by computing the error between the analytical and numerical solutions in the case of having an analytical solution. The absolute relative changes of the conservation laws can also be a good indicator to observe the validity and accuracy of the proposed method even when there exists no analytical solution. The scan to determine the optimum exponential B-spline parameter value shows that the accuracy of the solutions can be improved when compared the choice $\zeta = 1$.

6. Acknowledgements

This study is supported by Eskisehir Osmangazi University Scientific Research Projects Committee with project number 2016/19052. A brief part was orally presented at 3rd International Conference on Pure and Applied Sciences, Dubai, 2017.

References

References

- [1] Ruderman, M. S., Talipova, T., & Pelinovsky, E. (2008). Dynamics of modulationally unstable ion-acoustic wavepackets in plasmas with negative ions. *Journal of Plasma Physics*, 74(05), 639-656.
- [2] Kamchatnov, A. M., Kuo, Y. H., Lin, T. C., Horng, T. L., Gou, S. C., Clift, R., El, G.A., & Grimshaw, R. H. (2012). Undular bore theory for the Gardner equation. *Physical Review E*, 86(3), 036605.
- [3] Grimshaw, R., Pelinovsky, E., Taipova, T., & Sergeeva, A. (2010). Rogue internal waves in the ocean: long wave model. *The European Physical Journal Special Topics*, 185(1), 195-208.
- [4] Kamchatnov, A. M., Kuo, Y. H., Lin, T. C., Horng, T. L., Gou, S. C., Clift, R., El, G.A., Grimshaw, R. H. (2013). Transcritical flow of a stratified fluid over topography: analysis of the forced Gardner equation. *Journal of Fluid Mechanics*, 736, 495-531.
- [5] Slyunyaev, A. V., & Pelinovski, E. N. (1999). Dynamics of large-amplitude solitons. *Journal of Experimental and Theoretical Physics*, 89(1), 173-181.
- [6] Hu, H., Tan, M., & Hu, X. (2016). New interaction solutions to the combined KdV-mKdV equation from CTE method. *Journal of the Association of Arab Universities for Basic and Applied Sciences*, 21, 64-67.
- [7] Wei-Feng, Y., Sen-Yue, L., Jun, Y., & Han-Wei, H. (2014). Interactions between Solitons and Cnoidal Periodic Waves of the Gardner Equation. *Chinese Physics Letters*, 31(7), 070203.
- [8] Bekir, A. (2009). On traveling wave solutions to combined KdV-mKdV equation and modified Burgers-KdV equation. *Communications in Nonlinear Science and Numerical Simulation*, 14(4), 1038-1042.
- [9] Fu, Z., Liu, S., & Liu, S. (2004). New kinds of solutions to Gardner equation. *Chaos, Solitons & Fractals*, 20(2), 301-309.
- [10] Lü, H. L., Liu, X. Q., & Niu, L. (2010). A generalized (G'/G) -expansion method and its applications to nonlinear evolution equations. *Applied Mathematics and Computation*, 215(11), 3811-3816.

- [11] Naher, H., & Abdullah, F. A. (2012). Some new solutions of the combined KdV-MKdV equation by using the improved G/G-expansion method. *World Applied Sciences Journal*, 16(11), 1559-1570.
- [12] Taghizade, N., & Neirameh, A. (2010). The solutions of TRLW and Gardner equations by-expansion method. *Int. J. Nonlinear Sci*, 9(3), 305-310.
- [13] Akbar, M. A., Hj, N., & Ali, M. (2012). New solitary and periodic solutions of nonlinear evolution equation by Exp-function method. In *World Appl. Sci. J.*, 17(12), 1603-1610.
- [14] Wazwaz, A. M. (2007). New solitons and kink solutions for the Gardner equation. *Communications in nonlinear science and numerical simulation*, 12(8), 1395-1404.
- [15] Zayed, E. M. E., & Abdelaziz, M. A. M. (2012). The Two-Variable (G'/G, 1/G)-Expansion Method for Solving the Nonlinear KdV-mKdV Equation. *Mathematical Problems in Engineering*, 2012, Article ID 725061, 1-14.
- [16] Krishnan, E. V., Triki, H., Labidi, M., & Biswas, A. (2011). A study of shallow water waves with Gardner's equation. *Nonlinear Dynamics*, 66(4), 497-507.
- [17] Guo, Y. C., & Biswas, A. (2015). Solitons and other solutions to Gardner Equation by similarity Reduction. *Romanian Journal of Physics*, 60(7-8), 961-970.
- [18] Jawad, A. J. A. M. (2012). New Exact Solutions of Nonlinear Partial Differential Equations Using Tan-Cot Function Method. *Studies in Mathematical sciences*, 5(2), 13-25.
- [19] Hamdi, S., Morse, B., Halphen, B., & Schiesser, W. (2011). Conservation laws and invariants of motion for nonlinear internal waves: part II. *Natural hazards*, 57(3), 609-616.
- [20] Nishiyama, H., & Noi, T. (2016). Conservative difference schemes for the numerical solution of the Gardner equation. *Computational and Applied Mathematics*, 35(1), 75-95.
- [21] Rageh, T. M., Salem, G., & El-Salam, F. A. (2014). Restrictive Taylor Approximation for Gardner and KdV Equations. *Int. J. Adv. Appl. Math. and Mech*, 1(3), 1-10.
- [22] McCartin, B.J., *Theory of exponential splines*. *Journal of Approximation Theory*, **661**, 1-23, 1991.

- [23] Mohammadi, R., *Exponential B-Spline Solution of Convection-Diffusion Equations*. Applied Mathematics, **4**, 933-944, 2013.
- [24] Mohammadi, R., *Exponential B-spline collocation method for numerical solution of the generalized regularized long wave equation* Chin. Phys. B, **24** 5, 050206, 2015.
- [25] Ersoy, O., & Dag, I., *The exponential cubic B-spline algorithm for Korteweg-de Vries Equation* Advances in Numerical Analysis, Article ID 367056, 2015.
- [26] Ersoy, O., & Dag, I. (2016). *The Exponential Cubic B-Spline Collocation Method for the Kuramoto-Sivashinsky Equation*. Filomat, **30** 3, 853-861.
- [27] Dag, I., & Ersoy, O. (2016). *The exponential cubic B-spline algorithm for Fisher equation*. Chaos, Solitons & Fractals, **86**, 101-106.
- [28] Ersoy, O., & Dag, I. (2015). *Numerical solutions of the reaction diffusion system by using exponential cubic B-spline collocation algorithms*. Open Physics, **13**(1).
- [29] Rubin S. G. , Graves R. A., "Cubic spline approximation for problems in fluid mechanics", Nasa TR R-436, Washington, DC, (1975).